Research Paper https://doi.org/10.7733/jnfcwt.2022.021

Water Sorption/Desorption Characteristics of Eutectic LiCl-KCl Salt-Occluded Zeolites

Allison Harward[1], Levi Gardner[2], Claire M. Decker Oldham[1], Krista Carlson[3], Tae-Sic Yoo[4], Guy Fredrickson[4], Michael Patterson[4], and Michael F. Simpson[1,*]

[1]*University of Utah, 201 Presidents' Cir, Salt Lake City, UT 84112, USA*

[2]*Argonne National Laboratory, 9700 S Cass Ave, Lemont, IL 60439, USA*

[3]*University of Nevada at Reno, 664 N Virginia St, Reno, NV 89557, USA*

[4]*Idaho National Laboratory, 1955 N Fremont Ave, Idaho Falls, ID 83415, USA*

(Received June 8, 2022 / Revised June 24, 2022 / Approved June 29, 2022)

Molten salt consisting primarily of eutectic LiCl-KCl is currently being used in electrorefiners in the Fuel Conditioning Facility at Idaho National Laboratory. Options are currently being evaluated for storing this salt outside of the argon atmosphere hot cell. The hygroscopic nature of eutectic LiCl-KCl makes is susceptible to deliquescence in air followed by extreme corrosion of metallic cannisters. In this study, the effect of occluding the salt into a zeolite on water sorption/desorption was tested. Two zeolites were investigated: Na-Y and zeolite 4A. Na-Y was ineffective at occluding a high percentage of the salt at either 10 or 20wt% loading. Zeolite-4A was effective at occluding the salt with high efficiency at both loading levels. Weight gain in salt occluded zeolite-4A (SOZ) from water sorption at 20% relative humidity and 40°C was 17wt% for 10% SOZ and 10wt% for 20% SOZ. In both cases, neither deliquescence nor corrosion occurred over a period of 31 days. After hydration, most of the water could be driven off by heating the hydrated salt occluded zeolite to 530°C. However, some HCl forms during dehydration due to salt hydrolysis. Over a wide range of temperatures (320–700°C) and ramp rates (5, 10, and 20°C min^{-1}), HCl formation was no more than 0.6% of the Cl^- in the original salt.

Keywords: Zeolite, Electrorefiner salt, Ceramic waste form, Hydrolysis

*Corresponding Author.
Michael F. Simpson, University of Utah, E-mail: michael.simpson@utah.edu, Tel: +1-801-581-4013

ORCID

Allison Harward	http://orcid.org/0000-0003-4068-0293	Levi Gardner	http://orcid.org/0000-0002-7327-7620
Claire M. Decker Oldham	http://orcid.org/0000-0003-0003-4991	Krista Carlson	http://orcid.org/0000-0002-4288-2641
Tae-Sic Yoo	http://orcid.org/0000-0002-2244-5700	Guy Fredrickson	http://orcid.org/0000-0001-8711-338X
Michael Patterson	http://orcid.org/0000-0001-8245-2323	Michael F. Simpson	http://orcid.org/0000-0002-0099-0097

1. Introduction

Electrorefiners currently operating in the Fuel Conditioning Facility (FCF) of Idaho National Laboratory (INL) are being used to electrochemically process sodium bonded Experimental Breeder Reactor-II fuel using an electrolyte consisting of molten eutectic LiCl-KCl (58mol% LiCl, 42mol% KCl) with 5–10wt% UCl_3 [1-3]. These electrorefiners recover uranium metal from other elements present in the spent fuel (cladding, alloying zirconium, bond sodium, and fission products), allowing the uranium to be reused for fabricating new. As processing of sodium-bonded metal fuel occurs, the salt becomes increasingly concentrated with fission products, and it becomes necessary to either purify or dispose of the salt [3, 4].

Selectively removing fission products and sodium from the salt may prolong the useful lifetime of the salt. Means by which to accomplish this separation within reasonable cost are necessary for a sustainable electrorefining operation [oxygen bubbling, Li addition, Li_2O addition, phosphate addition, liquid cadmium cathode, etc.]. At times, operation conditions call for the retirement of the fraction or whole of the contaminated salt. Therefore, means by which to prepare contaminated salt for disposal or long-term storage are needed. Simply packaging the salt in sealed canisters and placing it in underground storage is unacceptable due to the hygroscopic behavior of the salt and accompanying enhanced corrosivity. The primary electrorefiner (ER) salt constituent, eutectic LiCl-KCl, absorbs water from the atmosphere readily to the point where it deliquesces [5]. The saline solution formed from such deliquescence is highly corrosive to steel alloys, typical canister materials storing the salt. Should the storage canister incur any leakage, the salt has the potential to hydrate and cause severe corrosion of the canister. This could lead to containment breech of radioactive fission products and actinides. While thermal processing of hydrated salt can return it to an anhydrous state, these processes require a chlorine potential to prevent the formation of oxychlorides which causes the formation of HCl [6].

One alternative to direct disposal of the ER salt is to first immobilize it in a ceramic waste form consisting of a composite of sodalite and borosilicate glass. Such a ceramic waste form (CWF) and a process for producing it were developed by Argonne National Laboratory and Idaho National Laboratory first under the Integral Fast Reactor program and then under the EBR-II spent fuel treatment program [7-11]. In this process, the salt is first occluded into dehydrated zeolite-4A and then undergoes pressureless consolidation with borosilicate glass frit [7-11]. Zeolite-4A is capable of absorbing chloride salt molecules within the available cavities of each unit cell due to the microporous channels created by the extra-framework cations and AlO_4 tetrahedra in the structure [12-15]. The zeolite structure is thermally stable above the melting temperature for the salt, making it suitable for the occlusion of salts as an immobilization measure [14, 16]. While the CWF process has been demonstrated at engineering scale, none of the needed equipment is currently installed in a hot cell at INL. The space needed in the hot cell for this process and time required for processing each batch are both very high [11].

To address placing ER salt into temporary storage, an option exists to simply occlude it in zeolite-4A and delay formation of final waste forms. This processing could be accomplished in the FCF with minimal new equipment. The purpose of performing this process would be to render the salt safe from deliquescence and prevent corrosion of the storage canisters. While zeolite-4A is the primary candidate for occluding the salt because of the extensive testing performed in development of the ceramic waste form, exploring alternative zeolites, whose capacity for salt occlusion may be greater, may be beneficial. Na-Y zeolite, of the faujasite family, was identified as one alternative zeolite to occlude the salt due to the large pore diameter (0.74 nm) and Si/Al ratio of 2.4, which should lower the affinity for water absorption [13, 14]. In comparison, the pore diameter of zeolite-4A is 0.4 nm and has a Si/Al ratio of 1. The

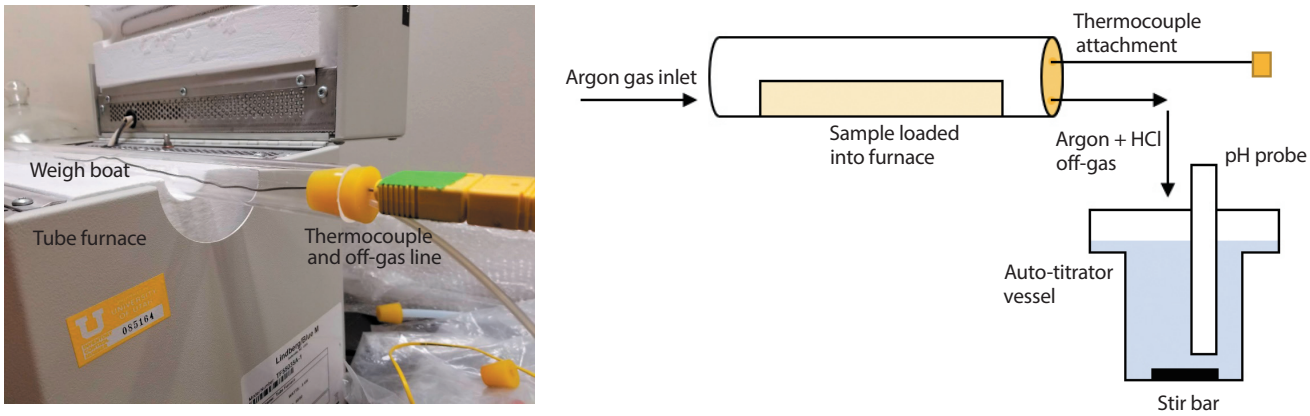

(a) (b)

Fig. 1. Dehydration testing tube furnace set-up (a) photo and (b) drawing with the thermocouple and off-gas line routed through the end. The argon and HCl off-gas flows into the auto-titrator vessel to measure rate of HCl flow out of the tube furnace.

H-exchanged variant of the ultra-stable Y zeolite (USHY) has been reported to be effective at absorbing simulant waste salt and generating HCl off-gas as a reaction product [17-19]. While the USHY ion exchange reaction with ER salt is a feasible approach to immobilize the salt for permanent disposal, this project sought treatment options avoiding off-gas handling to minimize operation complications.

In this project, sorption/desorption behavior of water in LiCl-KCl eutectic salt occluded zeolites (zeolite-4A and Na-Y) was studied to understand the benefit of using zeolites to enable storage of the salt in an environment which may involve contact with water vapor. The equilibrium uptake of water in salt occluded zeolite was measured, and the thermal desorption process was studied. Emphasis was placed on the minimization of HCl production during water desorption.

2. Materials and Methods

2.1 Materials

Zeolite-4A and Na-Y zeolite pellets (Riogen) were crushed and sieved to a size distribution of 45–250 μm (−60 +325 mesh). Salt composed of eutectic LiCl-KCl (58mol% LiCl, 42mol% KCl) was used to represent ER salt. The LiCl and KCl powders (reagent-grade, anhydrous; Fisher Scientific) were mixed into 40-g batches in an argon-atmosphere glove box with H_2O and O_2 levels kept at less than 10 ppm. The salt mixtures were loaded into glassy carbon crucibles (HTW Germany - Thierhaupten, Germany; H: 6.75”, OD: 1.75”), inside of the glove box the salts were heated at 10°C min^{-1}, held at 450°C for 60 minutes, and then left to cool slowly inside of the furnace. After cooling and removal from the crucibles, the salt was crushed and sieved to < 250-μm particle sizes in the glovebox.

2.2 Equipment

The hydration testing of salt occluded zeolite and dried zeolite-4A and Na-Y zeolite powders was done using an atmospheric humidity chamber (Test Equity Model TE-101H-F). Dry atmosphere work was done in a glovebox (Inert Technologies PureLab HE).

Dehydration testing was performed by loading 5-g samples of hydrated SOZ-4A into a quartz weigh boat and placed into a stationary tube furnace. Argon gas flowed through the inlet, and HCl gas produced during the experiments flowed through the outlet and into an auto-titrator vessel where the pH change was measured over time. This

set up is pictured in Fig. 1(a) and illustrated in Fig. 1(b).

2.3 Procedures

Hydration experiments were performed with 1.50 ± 0.00 g zeolite samples and 40.00 ± 0.01 g salt occluded zeolite (SOZ) samples placed in petri dishes and glass beakers, respectively. Samples were exposed to 20 ± 3% relative humidity (RH) at 40 ± 0.5°C, and mass measurements were recorded to determine water uptake as a function of time. To characterize the effects of salt-occluded zeolite on stainless steel, 5 ± 0.05 g samples were held in 10-mL stainless steel crucibles during hydration, and photos were taken over time to document any visible degradation to the crucible.

Prior to salt occlusion, batches of 60 to 70 g of each zeolite 4A and Na-Y were loaded into alumina crucibles and dehydrated by heating at 5°C min^{-1} to 500°C in a furnace located in the glovebox. Batches were combined and characterized to provide a consistent source of dried zeolite to be used for preparing salt-occluded zeolite and supporting further experimentation.

Salt occlusion was performed by mixing LiCl-KCl powder with the dried zeolites in 10-g batches (duplicate batches were loaded to 10 and 20 mass% salt). Occlusion reactions were run by loading a pre-mixed batch into an alumina crucible, heating to 500°C (zeolite-4A) or 625°C (zeolite Na-Y) at 5°C min^{-1} and holding for 24 h. The higher temperature for occlusion in Na-Y was used based on work previously published by Wasnik et. al [18]. The zeolite-salt mixtures were periodically removed from the furnace and stirred for 60 s. This procedure was completed four times for each batch. The mixture was then cooled inside the furnace for five hours. This procedure was performed inside of the glove box.

Dehydration experiments were performed to determine the extent of HCl production. Hydrated SOZ samples were loaded into a quartz weigh boat and placed into the center of the horizontal tube furnace. Argon gas flowed through the furnace at a rate of 67 cm^3 min^{-1}. A thermocouple was inserted into the tube and placed close to the sample for accurate temperature readings. Effluent gas was routed to the auto-titrator cell where any HCl was titrated with measured volumes of 0.05 M NaOH to maintain a constant pH of 10. Table 1 outlines the sample matrix used for these experiments.

Table 1. List of dehydration experiments with conditions. All tests were run with a batch of SOZ containing 20.0 g of LiCl-KCl and 80.0 g of dehydrated zeolite-4A. Target hold temperature was 510−520°C. Actual observed maximum temperatures are given for most runs in the table

Sample ID	Sample Mass (g)	Ramp Rate (°C min^{-1})	Maximum T (°C)
5C1	5.50	5	528
5C2	5.51		528
5C3	5.51		526
10C1	5.54	10	532
10C2	5.52		534
10C3	5.51		not available
20C1	5.57	20	537
20C2	5.54		536
20C3	5.49		not available

2.4 Material Characterization

The moisture content within zeolite and SOZ samples was measured using a simultaneous thermal analyzer (STA) (TA Instruments Model SDT-650). Samples were prepared in the argon atmosphere glovebox. To minimize contact with air the samples were loaded into alumina sample pans inside of the glove box and loaded into sealed glass vials. The vials were transferred out of the glovebox and moved to the STA when it was ready to receive the sample. The vials were open, and the pans containing the samples were quickly loaded into the STA, which was closed quickly with flowing ultra-high purity argon gas at 50 ml min^{-1}.

The STA was programmed to heat the samples to 600°C at 10°C min^{-1}, under ultra-high-purity argon gas (50 cm^3 min^{-1}). The weight loss of the sample is assumed to be water off-gassing from the sample.

Free chloride analysis was conducted on each sample to assess the degree of occlusion achieved in each batch. This process involved mixing 0.5 g of SOZ with 25 mL of purified, deionized water. This mixture was agitated by hand for 60 s and immediately filtered through a 0.45 μm filter. An ion-selective probe (Thermo Scientific Orion 9617BNWP) was used to measure the resulting free Cl^- concentration in the solution.

X-ray diffraction (XRD) (Rigaku Miniflex600) was performed at ambient temperature (approximately 20°C) on SOZ powders following dehydration to ensure that the crystallinity was maintained. Measurements were run over a range of 2–70° 2θ with a step size of 0.02° and at a scan rate of 3° min^{-1}.

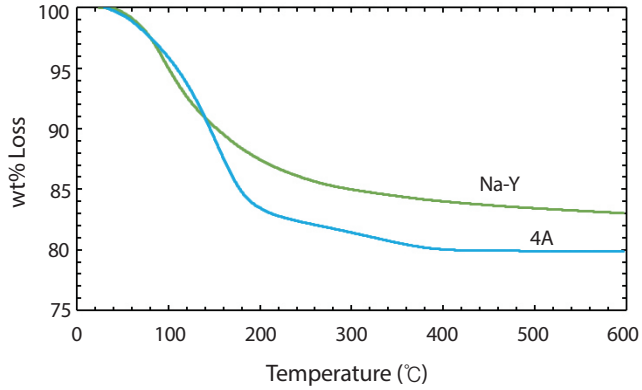

Fig. 2. Thermal dehydration curves for zeolites-4A (20.15wt% maximum loss at 600°C) and Na-Y (16.98wt% maximum loss at 600°C) as measured via STA (10°C min^{-1} to 600°C). Both materials were initially equilibrated with water vapor at 20% RH, 40°C.

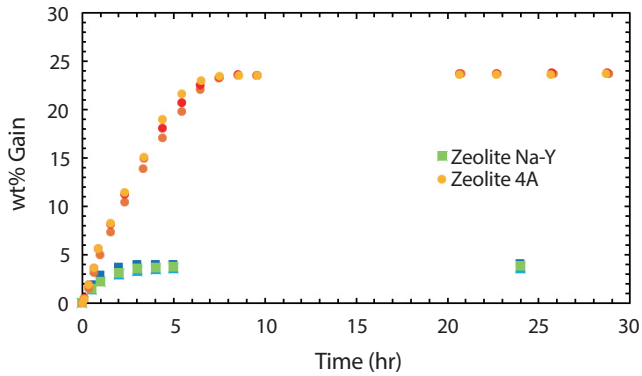

Fig. 3. Water uptake curves for zeolites previously dried at 500°C (zeolite-4A) and 625°C (zeolite Na-Y). Replicates of zeolite 4A are seen as the top curve which equilibrates at 23.82 ± 0.04wt% and zeolite Na-Y replicates as the bottom curve which equilibrates at 3.81 ± 0.22wt%.

3. Results and Discussion

3.1 Zeolite Hydration

Mass loss and gain experiments were performed to determine the water sorption characteristics in zeolites-4A and Na-Y absent of occluded salt in order to compare the affinity of these zeolites for water. It is understood that water uptake in a salt occluded zeolite can be affected by properties of both the salt and the zeolite. An ideal sorbent for protecting the salt from uptake of water would have a high affinity for salt but a low affinity for water. Fig. 2 shows the mass loss due to thermal dehydration of samples of zeolite-4A and Na-Y that had been saturated in the humidity chamber (see section 2.3) after receipt from the supplier. As can be seen in Fig. 2, a greater weight loss was observed for zeolite-4A (20.15wt%) than zeolite Na-Y (17.0wt%) during heating to 600°C. Next, samples of zeolites 4A and Na-Y that had been dehydrated at 500°C were placed in the humidity chamber, and their masses were recorded over the time needed to reach equilibrium. Fig. 3 shows the relative mass gain for these two zeolites over a period of about 43 h. While Fig. 2 also showed that zeolite 4A absorbs more water than zeolite Na-Y, the amount of water sorption of zeolite Na-Y was much less than the amount of water desorption. The weight loss of hydrated zeolite Na-Y was 17.0%, while the weight gain was only 3.81%. The weight gain number can be used to calculate an equilibrium water content in zeolite Na-Y of 3.7wt%. Published values of equilibrium uptake of H_2O in zeolite

Table 2. 10 and 20wt% LiCl-KCl was occluded into dehydrated zeolites 4A and Na-Y, the percent of salt successfully occluded into each zeolite is listed

wt% LiCl-KCl in Mixture	% Occlusion into Zeolite-4A	% Occlusion into Zeolite Na-Y
10.0	99.4	69.2
20.0	99.3	17.1

Na-Y are actually comparable to that of zeolite-4A [14], lending more credence to the results shown in Fig. 2. One possible explanation is that the Na-Y was overheated, and some thermal degradation occurred which prevented the normal rehydration of water.

3.2 Occlusion of LiCl-KCl in Zeolite-4A and Na-Y

The two zeolite options for stabilizing the salt for long term storage were dehydrated and tested for occlusion by LiCl-KCl eutectic to determine occlusion capacity. Two salt occlusion levels (10 and 20wt%) were used in tests. The lower level was selected based on specified electrorefiner salt loading in zeolite-4A in the baseline glass-bonded sodalite waste process developed by Argonne National Laboratory [11]. The higher level was based on the theoretical occlusion limit of 12 Cl^- per pseudo unit cell ($Na_{12}(SiO_2)_{12}(AlO_2)_{12}$) in zeolite-4A [9]. Occlusion tests were run as described in section 2.3. The free chloride analyses [5] were used to calculate the percentage of salt that was occluded (i.e., resists dissolution in a quick rinse in water), and those results are shown in Table 2. Zeolite 4A occludes over 99% of the salt both at 10 and 20wt% loading, while zeolite Na-Y occludes no higher than 69% of the salt. It was concluded that dehydrated zeolite Na-Y has a much lower retention capability of LiCl-KCl than zeolite 4A. We recall that dehydration of zeolite Na-Y manifested a much-lowered water uptake capacity, hinting structural damage. Though salt occlusion capability of zeolite Na-Y is inconclusive, zeolite Na-Y was eliminated as a candidate zeolite for this application and is not further analyzed or discussed in this paper.

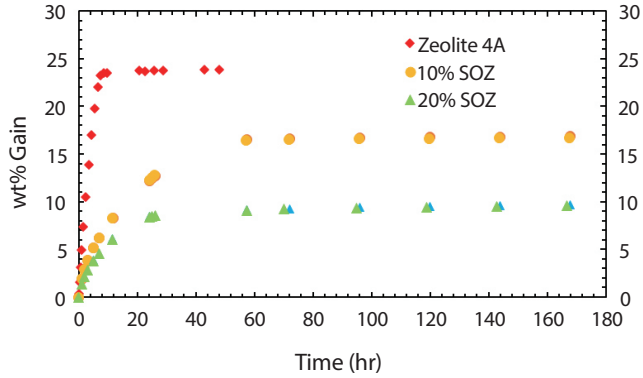

Fig. 4. Hydration curves for 10% SOZ-4A and 20% SOZ, alongside the dried and un-occluded counterpart, zeolite-4A, for reference. Duplicates of 10% SOZ are seen as the middle curve which equilibrates at 17.0 and 16.9wt% and 20% SOZ duplicates as the bottom curve which equilibrates at 10.4 and 10.2wt%.

3.3 Hydration of LiCl-KCl Occluded Zeolite-4A

With the focus on zeolite-4A as the prime candidate to occlude ER salt, a series of hydration tests were performed in the humidity chamber. The hydration curve for 10 and 20wt% SOZ-4A is plotted alongside the un-occluded zeolite counterpart in Fig. 4. Fig. 4 gives the percentage mass increase, starting with dehydrated samples. This plot shows that the salt occlusion process reduces the affinity of the zeolite for water, likely due to the available zeolite pore space becoming partially filled with LiCl-KCl salt. This data was used to calculate the fraction of water in the equilibrated, water-hydrated samples. The equilibrium water content in the zeolite 4A was reduced from 19.4 to 8.3wt% as a result of occlusion of 20wt% LiCl-KCl. Another important consideration is the effect of occlusion by the zeolite on hydration of the salt. Water absorbed in SOZ could be assigned to the zeolite or the salt. Mass change measurements cannot differentiate between the two. In a recent publication, our group

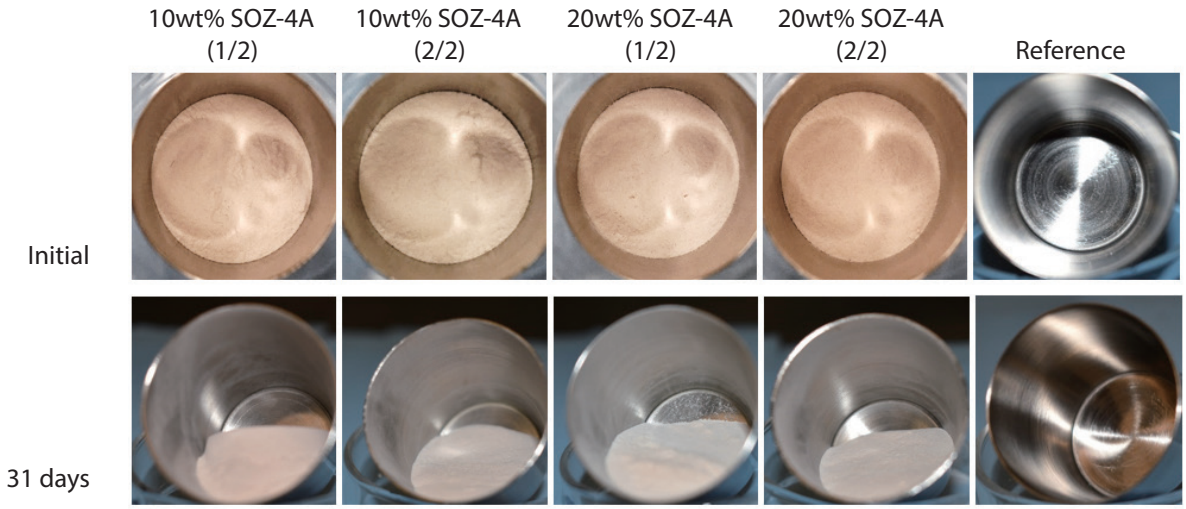

Fig. 5. Images of SOZ-4A before and after hydration.

Table 3. Total wt% gain of three samples from a 20% SOZ-4A batch were prepared in the HC alongside the wt% loss during TGA of each respective subsample

	Sample 1	Sample 2	Sample 3	Average
wt% gain (HC)	9.82	9.56	9.74	9.71 ± 0.14
wt% loss (TGA)	9.08	9.05	9.16	9.10 ± 0.058

reported that hydrated eutectic LiCl-KCl contained 40wt% H_2O at 40°C, 20% RH [5]. Hydration was tested in SOZ and reported in Fig. 4 with the same conditions. Based on 8.3wt% water in SOZ with 20wt% salt and all of the water being associated with the salt, the salt would contain 31wt% H_2O. Therefore, the effect of occluding the salt into zeolite 4A on its hydration capacity is a small reduction. Fig. 6 shows photos of SOZ-4A samples taken before and after hydration. Even after equilibrating with water vapor for nearly 200 h, there was no visual evidence of deliquescence or stainless-steel container corrosion. This shows that SOZ-4A can be stored in a stainless-steel container under humid atmosphere without severe consequences. Our team previously reported that deliquescence was observed on eutectic LiCl-KCl under the same conditions within 17 h [5].

3.4 Dehydration of Hydrated, LiCl-KCl Occluded Zeolite-4A (SOZ-4A)

Table 3 gives the percentage weight gained by SOZ-4A samples in the humidity chamber (HC) and the percentage weight loss as measured via STA. The average gain in the HC was 9.7%. The complicating factor is that mass loss can be due to H_2O desorption and/or HCl off-gas. If the entirety of the weight gain was attributed to water, that corresponds to the hydrated SOZ-4A having a water content of 8.8wt%. However, the average weight loss measured by TGA was 9.1wt%. Assuming that the residual water after running a dehydration cycle is fixed, the difference in these two numbers suggests that some HCl may be produced during thermal dehydration. Ideally, the weight percentage lost would equal the weight percentage of water. But it does insinuate

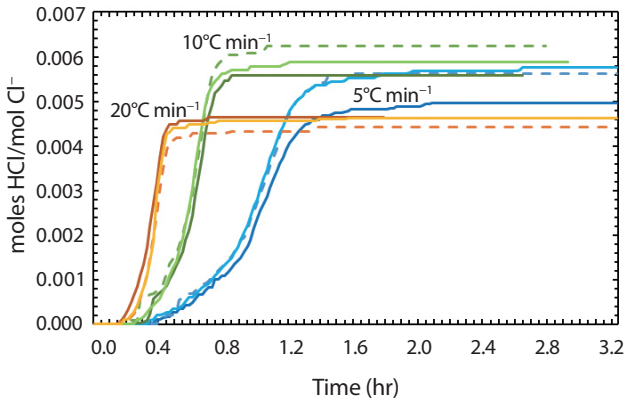

Fig. 6. Moles of HCl generated per mole of Cl^- at ramp rates 5, 10, and 20°C min^{-1} (held at 530°C) is plotted versus time. Samples used for dehydration were 20% SOZ-4A previously hydrated by ~11wt%.

additional weight loss due to Cl^- ions in the salt. Up to two moles of HCl could be off gassed in lieu of one mole of water, as shown below. The small difference in estimated water content and weight loss suggests that this should be a minor reaction. The HCl generation question is further investigated below.

The following reactions of salts with water could potentially result in formation of volatile HCl during dehydration.

$$H_2O + 2LiCl = Li_2O + 2HCl$$
$$H_2O + LiCl = LiOH + HCl$$
$$H_2O + KCl = K_2O + 2HCl$$
$$H_2O + KCl = KOH + HCl$$

In order to detect/measure HCl generation, experiments were run in which 5 g samples of ~10% hydrated 20%-SOZ-4A were heated in a tube furnace with the carrier gas directed into an auto-titrator that reacted any HCl injected into the cell with equimolar amounts of NaOH to automatically keep the pH at 10. As shown in Fig. 6, HCl was consistently measured based on the auto-titrator output in every dehydration experiment with maximum temperature ranging from 320 to 700°C. Fig. 6 shows the effect of temperature ramp rate on the HCl production versus time and Fig. 7 includes the temperature profile each run followed. In each experiment, the maximum temperature was ~530°C. It was expected that increasing the ramp rate would increase HCl production. Higher ramp rates did cause the HCl to be produced quicker, but there was no

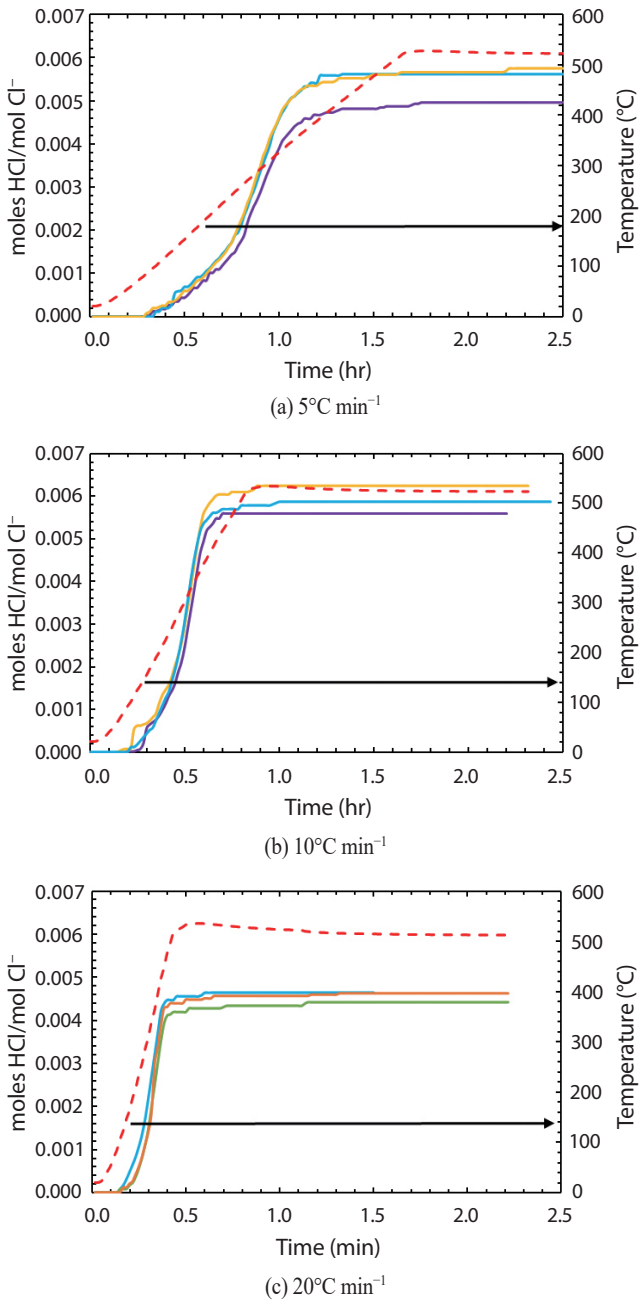

Fig. 7. The same HCl generation data in Fig. 7 is plotted with their respective temperature profiles, seen as the red dotted lines with the arrow pointing towards the temperature axis. Each run for ramp rates 5, 10, and 20°C min^{-1} are plotted in (a), (b), and (c), respectively.

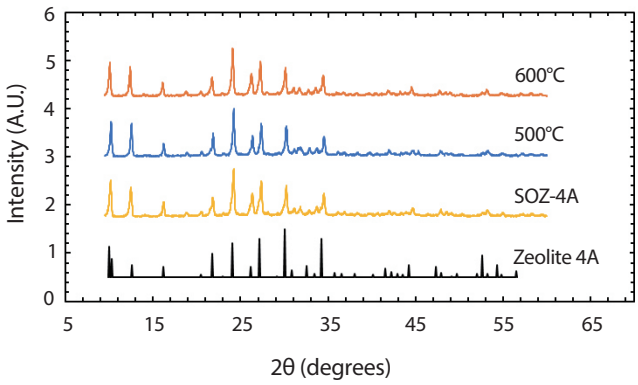

Fig. 8. XRD patterns for dehydrated SOZ-4A samples in addition to zeolite-4A and SOZ-4A not subjected to hydration and dehydration.

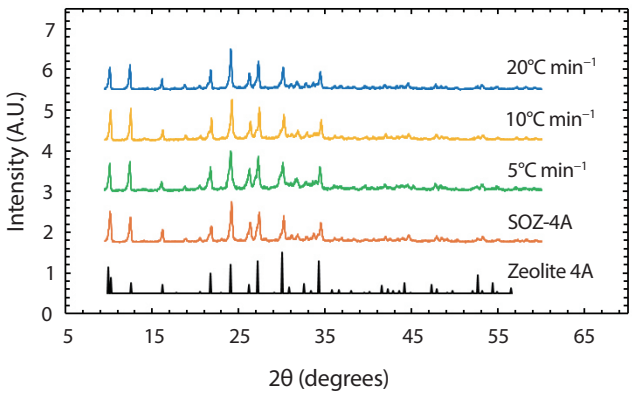

Fig. 9. XRD patterns for dehydrated 20% SOZ-4A samples from tests with varying ramp rates (5°C min^{-1}, 10°C min^{-1}, and 20°C min^{-1}) to 530°C.

consistent trend for total HCl versus ramp rate. The least HCl was produced at the highest ramp rate (20°C min^{-1}).

XRD patterns of zeolite samples heated to as high as 600°C to reverse the hydration are shown in Figs. 8 and 9, alongside a reference pattern for zeolite-4A and SOZ 4A. Both figures indicate that the zeolite structure remains stable under ramp rates up to 20°C min^{-1} and hold temperatures up to 600°C. Given that free-flowing powder is unattractive for final disposal, it is desirable to be able to further process the SOZ later into a solid, durable waste form such as the glass bonded sodalite waste form [11]. The data shown here indicates that the SOZ 4A can be completely dehydrated after some period of storage and slow sorption of water and then be consolidated at high temperature with glass frit into waste forms.

5. Conclusions

This work shows a feasible pathway for storing of ER waste salt outside of an inert atmosphere temporarily. Zeolite-4A and zeolite Na-Y were tested for occluding up to 20wt% eutectic LiCl-KCl. Na-Y was found to be ineffective at occluding the salt at target levels of either 10 or 20wt%. Zeolite-4A was found to be a suitable material to occlude the salt and prevent it from deliquescing in water and causing corrosion of stainless metal cannisters used for storage. Equilibrium water content in 20wt% LiCl-KCl occluded zeolite-4A is significantly reduced compared to zeolite-4A without any salt occluded. By comparing the results of this study to our previous work on water vapor sorption in eutectic LiCl-KCl, we can conclude that occlusion by zeolite reduces the capacity for the salt to hydrate. Water absorbed by the SOZ can be thermally dehydrated by heating at a range of 5 to 20°C min^{-1} to 600°C. Less than 0.6% of the salt is hydrolyzed to form HCl from this thermal treatment. While previous work showed that LiCl-KCl deliquesced at 40°C, 20% RH in 17 h, neither deliquescence nor corrosion occurs with LiCl-KCl occluded zeolite-4A samples under these conditions for upwards of 31 days. The zeolite maintains a crystalline structure during dehydration below 600°C, supporting the idea that the waste material could later be converted into a glass bonded sodalite waste form.

Acknowledgements

This work was supported by Idaho National Laboratory under standard subcontract no. 244567 and performed under the auspices of the U.S Department of Energy Fuel Cycle Research and Development Program. Idaho National Laboratory is operated by Battelle Energy Alliance, LLC under contract no. DE-AC07-05ID14517.

REFERENCES

[1] C.E. Till, Y.I. Chang, and W.H. Hannum, "The Intergral Fast Reactor-an Overview", Prog. Nucl. Energy, 31(1-2), 3-11 (1997).

[2] J.J. Laidler, J.E. Battles, W.E. Miller, and E.C. Gay, "Development of IFR Pyroprocessing Technology", Conference: Global '93: Future Nuclear Systems – Emerging Fuel Cycles and Waste Disposal Options, Conf-930913-40, September 12-17, 1993, Seattle.

[3] G.L. Fredrickson, M.N. Patterson, D. Vaden, G.G. Galbreth, T.S. Yoo, J.C. Price, E.J. Flynn, and R.N. Searle, "History and Status of Spent Fuel Treatment at the INL Fuel Conditioning Facility", Prog. Nucl. Energy, 143, 104037 (2022).

[4] M.F. Simpson, M.N. Patterson, J. Lee, Y. Wang, J. Versey, and S. Phongikaroon, "Management of Salt Waste From Electrochemical Processing of Used Nuclear Fuel", Conference: Global 2013, INL/CON-13-28041, INL, Salt Lake City, Utah (2013).

[5] L. Gardner, A. Harward, J. Howard, G. Fredrickson, T.S. Yoo, M.F. Simpson, and K. Carlson, "Deliquescence of Eutectic LiCl-KCl Diluted With NaCl for Interim Waste Salt Storage", Nucl. Technol., 208(2), 310-317 (2022).

[6] W.J. Burkhard and J.D. Corbett, "The Solubility of Water in Molten Mixtures of LiCl and KCl", J. Am. Chem. Soc., 79(24), 6361-6363 (1957).

[7] D. Lexa, L. Leibowitz, and J. Kropf, "On the Reactive Occlusion of the (Uranium Trichloride + Lithium Chloride + Potassium Chloride) Eutectic Salt in Zeolite 4A", J. Nucl. Mater., 279(1), 57-64 (2000).

[8] C. Pereira, M.A. Lewis, and J.P. Ackerman, "Overview of Mineral Waste Form Development for the Electrometallurgical Treatment of Spent Nuclear Fuel", Argonne National Laboratory, ANL/CMT/CP-88394 (1996).

[9] C. Pereira, M. Hash, M. Lewis, and M. Richmann, "Ceramic-composite Waste Forms From the Electrometallurgical Treatment of Spent Nuclear Fuel", JOM, 49(7), 34-40 (1997).

[10] K. Carlson, L. Gardner, J. Moon, B. Riley, J. Amoroso, and D. Chidambaram, "Molten Salt Reactors and Electrochemical Reprocessing: Synthesis and Chemical Durability of Potential Waste Forms for Metal and Salt Waste Streams", International Materials Reviews, 66(5), 339-363 (2021).

[11] M.C. Morrison, K.J. Bateman, and M.F. Simpson, "Scale up of Ceramic Waste Forms for the EBR-II Spent Fuel Treatment Process", International Pyroprocess Research Conference, INL/CON-10-19439, INL, Dimitrovgrad, Russia (2010).

[12] M.V. Šušić, N.A. Petranović, and D.A. Mioč, "The Properties of Zeolite 4A Treated in Molten Salts", J. lnorg. Nucl. Chem., 33(8), 2667-2675 (1971).

[13] H.S. Sherry, "The Ion-Exchange Properties of Zeolites. I. Univalent Ion Exchange in Synthetic Faujasite", J. Phys. Chem., 70(4), 1158-1168 (1966).

[14] D.W. Breck, Zeolite Molecular Sieves: Structure, Chemistry, and Use, John Wiley & Sons, New York (1974).

[15] S.M. Auerbach, K.A. Carrado, and P.K. Dutta, Handbook of Zeolite Science and Technology, Marcel Dekker, Inc., New York (2003).

[16] G. Cruciani, "Zeolites Upon Heating: Factors Governing Their Thermal Stability and Structural Changes", J. Phys. Chem. Solids, 67(9-10), 1973-1994 (2006).

[17] P. Bagri and M.F. Simpson, "Occlusion and Ion Exchange of Eutectic LiCl-KCl in H-Y Zeolite", J. Nucl. Fuel Cycle Waste Technol., 13(S), 45-53 (2015).

[18] M.S. Wasnik, A.K. Grant, K. Carlson, and M.F. Simpson, "Dechlorination of Molten Chloride Waste Salt From Electrorefining Via Ion-exchange Using Pelletized Ultra-stable HY Zeolite in a Fluidized Particle Reactor", J. Radioanal. Nucl. Chem., 320(2), 309-322 (2019).

[19] M.S. Wasnik, T.C. Livingston, K. Carlson, and M.F. Simpson, "Kinetics of Dechlorination of Molten Chloride Salt Using Protonated Ultra-stable Y Zeolite", Ind. Eng. Chem. Res., 58(33), 15142-15150 (2019).